

Horizontal and Vertical Structure of the Gulf Stream Velocity Field at 68°W

MELINDA M. HALL

Scripps Institution of Oceanography, La Jolla, CA 92093

(Manuscript received 13 August 1985, in final form 3 February 1986)

ABSTRACT

A current meter mooring, instrumented from the bottom into the thermocline, was deployed in the Gulf Stream at 68°W for a year. Data from the uppermost instrument indicate the Gulf Stream moved back and forth across the mooring site, so that the horizontal as well as vertical structure of the Stream may be deduced. The two key points to the success of the analysis are: 1) the well-defined relationship between temperature and cross-stream distance in the thermocline, enabling the use of the former as a horizontal coordinate; and 2) a daily-changing definition of Gulf Stream flow direction based on the shear between the thermocline and 2000 m depth. Time-series of daily-rotated velocities may be used to calculate empirical orthogonal functions for the along- and cross-stream vertical structures, which are decoupled and are respectively baroclinic and barotropic. Using the inferred horizontal coordinate one can estimate mass, momentum and kinetic energy fluxes for four individual events when the entire Stream swept by the mooring. The results for mass fluxes agree well with historical data. Bryden's method has been used to calculate vertical velocities from the temperature equation; the resulting time-series of w are visually coherent throughout the water column and their vertical amplitude structure looks like that of a first baroclinic mode. The rms vertical velocities are large [$O(0.05 \text{ cm s}^{-1})$], and these as well as other estimates have been used to explore the validity of the quasi-geostrophic approximation at the mooring site. The Rossby number for the thermocline flow is about 0.3, and for the deep flow is ≤ 0.1 .

1. Introduction

Although the Gulf Stream is one of the most heavily documented features in the deep North Atlantic, it is also terribly complicated, and continues to defy complete understanding. Part of the problem lies in the type of observations that have been feasible in the Gulf Stream. Hydrographic surveys such as Gulf Stream '60 (Fuglister, 1963) have served to define the baroclinic structure rather well, but since that study had but a few float trajectories to aid in choice of a reference level for geostrophic velocities, the barotropic aspects of the flow remained largely unknown. Moreover, a hydrographic survey is at best a snapshot of the flow in time. In recent years the surface thermal front has been monitored by satellite, producing continuous long time-series of front position (subject to cloud cover, of course); but a clear relationship between the Gulf Stream surface expression and the flow at depth has not yet been established. The deployment of large numbers of floats over the past decade has helped in describing gross features of the Gulf Stream's time variability—e.g., how meanders and eddies affect the eddy kinetic energy patterns at various depths in the North Atlantic (Richardson, 1983a)—but because there is little control over the floats after deployment, it has been virtually impossible to learn how the baroclinic structure itself varies with time. Clearly this aspect must be monitored by long-term fixed moorings with instruments throughout the water column; only recently

has the technology become available for the successful deployment of such moorings.

From October 1982 to October 1983 a current meter mooring reaching from the bottom into the thermocline was deployed for the first time in the Gulf Stream at 68°W. Because this was a pilot experiment for future work, only a single mooring was deployed; hence, careful interpretation of the data is required. In fact, the temperatures, pressures, and velocities at the uppermost instrument indicate the Gulf Stream moved back and forth across the mooring site, so that the entire Stream was sampled in time, and the data may be used to examine horizontal as well as vertical structure of the Stream. Furthermore, the well documented baroclinic structure of the Stream may be used to infer an instantaneous "streamwise direction of flow." That is, the Gulf Stream is recognized as a permanent front that may change its orientation, with quasi-permanent attributes such as strong vertical shear of the flow velocity. It will be demonstrated that there is a clear distinction between the "average Gulf Stream" as determined in Stream coordinates, and Eulerian mean flow at the mooring site.

In section 2 the observational program is discussed briefly. Then section 3 presents the vertical structure of the Eulerian mean flow at the mooring site, as well as of the average Gulf Stream, and places the results in the context of past work. In section 4 the machinery is developed to extract horizontal information from the dataset, allowing estimates of mass, momentum

and kinetic energy transports. This machinery further enables the calculation of vertical velocities from the temperature equation in section 5. Finally, in section 6, the validity of the quasi-geostrophic approximation at the mooring site is assessed.

2. Observational program

The GUSTO mooring (*Gulf Stream Observations*) was deployed for one year at 37°37'N, 68°00'W, the mean position of the Gulf Stream at that longitude (Halliwell and Mooers, 1983). Currents, temperature, and pressure were recorded at the nominal deployment depths of 400, 700 and 1000 m, while current and temperature only were measured at 2000 and 4000 m. The only missing data are at the middle instrument (1000 m), where the VACM stopped working after 64 days, but resumed after 56 more days. The time series were low-pass filtered with a 24-hr Gaussian filter, then sub-sampled daily, resulting in 360 days of data for all but the 1000 m level. Inspection of the National Weather Service analyses of satellite data, indicating the approximate surface expression of the Gulf Stream as determined by the surface thermal front, shows that the mooring was in the Stream 58 percent of the time, in the Slope Water to the north 12 percent of the time, and Sargasso water to the south 30 percent of the time. During the entire deployment period, no Gulf Stream rings were observed at the mooring position in the satellite analyses.

The strong currents tilted the mooring: average pressure at the top instrument was 498 db, with a minimum of 433 db and a maximum of 680 db. Thus, to create time series that could be used in a consistent manner, velocities were linearly interpolated or extrapolated to intermediate standard pressures of 575, 875 and 1175 db, while temperatures were corrected to those depths using a scheme described in Raymer et al. (1984). The same gap exists in the time series at 1175 db as in that at the 1000 m instrument.

3. Vertical structure at the mooring site

a. Mean statistics of the Eulerian flow

Table 1 shows the record-length mean east and north velocities and temperatures at the five standard depths. Also shown are the variances of these quantities. In

spite of the often large deviation from east of the current direction at 575 db, the mean velocity there is directed essentially due east. It is, however, much smaller than the maximum speeds recorded there, which are well over 100 cm s⁻¹. Mean northward velocities throughout the water column are extremely small and are nearly depth-independent, though on a daily basis there may be considerable shear in that direction (Fig. 1a). Since *v* is barotropic while *u* is baroclinic, the mean velocity vectors turn cyclonically going from deep to shallow, implying a mean downward vertical velocity (Bryden, 1980) due to the presence of the mean field. The mean velocity at 4000 m is directed nearly along-isobath, which is about 70° true (bottom depth is 4688 m), and the average zonal velocity there is westward rather than eastward. This deep flow is reminiscent of what Luyten (1977) found in his “upper rise” regime at 70°W, with along-isobath flow directed mostly westward. The mean temperature at 575 db is very close to that associated with the Gulf Stream axis, as discussed in section 4, suggesting that this was indeed the average location of the Stream for the year.

The eddy kinetic energy (EKE) is surface intensified for both components, indicating the baroclinicity associated with the Gulf Stream appears in north as well as east velocities. Magnitudes and vertical structure of EKE from Table 1 may be compared with Richardson’s (1983b) results for a vertical section of EKE along 55°W, constructed from drifter, float and current meter data. In that section, values range from roughly 500 cm² s⁻² at 575 db, to values of 130 to 140 cm² s⁻² for depths greater than 1500 m. The values in Table 1 show slightly stronger depth-dependence, ranging from 1050 cm² s⁻² at 575 db to 108 cm² s⁻² at 1175 db, then decaying moderately to deep values of 55–70 cm² s⁻². Schmitz (1984) also found that the variation of EKE with depth is much less in deep water than shallow. He found abyssal (4000 m) values near the Gulf Stream at 70°W of 104 cm² s⁻², about midway between the Table 1 values of 58 cm² s⁻² and Richardson’s (1983b) value of 138 cm² s⁻².

b. Vertical structure of the “average Gulf Stream”

In order to obtain a description of the Gulf Stream as a discrete feature from the flow at the current meter

TABLE 1. Record-length statistics for east and north velocity and temperature corrected time series at the “standard” depths (see text).

Depth (db)	Days of data	\bar{u} (cm s ⁻¹)	\bar{v} (cm s ⁻¹)	\bar{T} (°C)	$\overline{u^2}$ (cm ² s ⁻²)	$\overline{v^2}$ (cm ² s ⁻²)	$\overline{T^2}$ (°C ²)
575	360	38.402	-0.952	12.598	1487.63	601.95	16.936
875	360	17.320	-1.042	7.635	438.33	192.03	5.840
1175	240	6.906	-0.809	4.880	126.87	89.65	0.572
2000	360	4.816	-0.944	3.711	68.65	67.18	0.028
4000	360	-1.038	-0.599	2.311	54.16	61.79	0.001

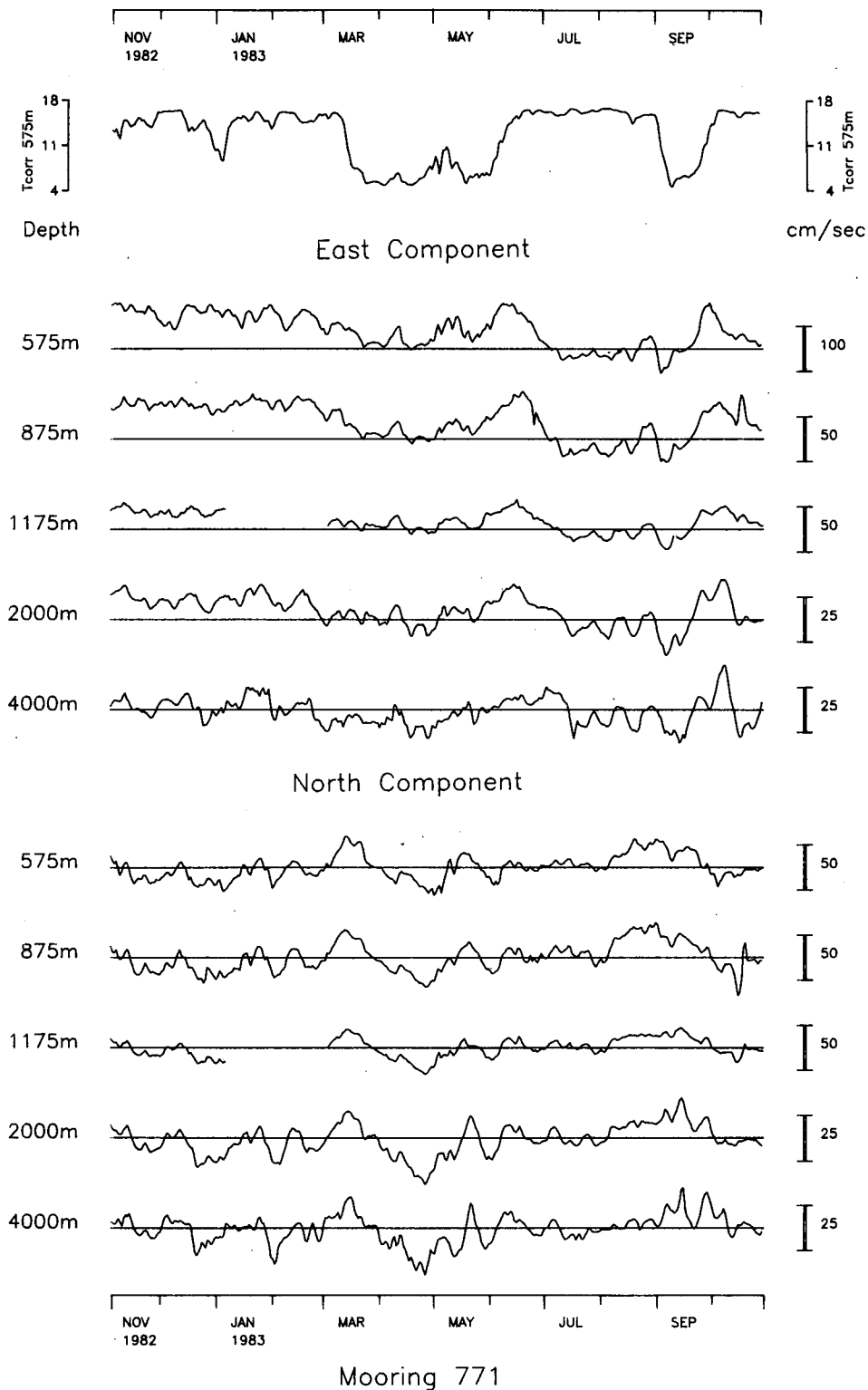


FIG. 1. (a) Time series of east (top) and north (bottom) velocities at five standard depths; (b) flow direction, defined as direction of shear between 400 and 2000 m instruments; due east is the zero line; (c) time series of along- and cross-stream velocities (see text) at five standard depths; cross-stream velocities are positive when 90 deg to the left of positive alongstream velocities. At top is time series of T_{575} , temperature corrected to 575 db.

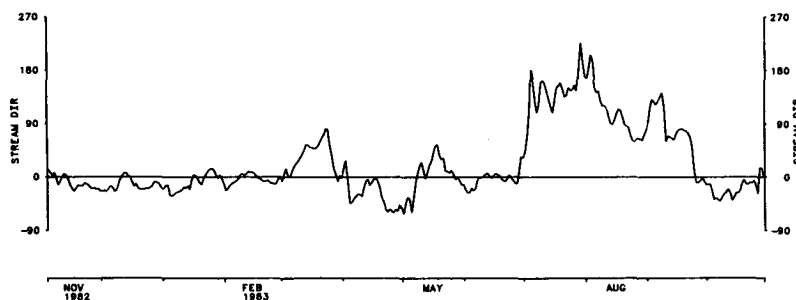


FIG. 1. (Continued)

site, a definition of what direction the Stream is flowing at any given time is required because, as the Gulf Stream meanders and changes direction, a significant part of the "alongstream" flow may be contained in the northward component of velocity. The direction of shear between the measured current at the uppermost (400 m) instrument and that at the 2000 m instrument has been chosen as the definition of the alongstream flow direction. Other definitions were examined as well, such as the shear direction between 400 and 700 m, or between 400 and 4000 m. These results do not differ much from those obtained for shear direction between 400 and 2000 m. However, because strong vertical shear has long been recognized as a signature of Gulf Stream flow, it seemed desirable to account for as much of the signal as possible in the "alongstream" definition, while avoiding problems with flow reversals at 4000 m, such as the bottom intensified westward flow in early April (Fig. 1a). The alongstream direction is shown as a function of time in Fig. 1b, with zero corresponding to due East.

The time series of along- and cross-stream velocities are shown in Fig. 1c, along with T_{575} (temperature corrected to 575 db). Positive cross-stream velocities correspond to flow 90 degrees to the left of alongstream velocity. A monotonic increase or decrease in T_{575} signals the passage of the Gulf Stream across the mooring site: four clear examples occur in March, June, late August/early September, and later September. The Gulf Stream also occupied the mooring site for long periods when it did not sweep completely across, such as from November 1982 to March 1983. Comparison of Figs. 1a and 1c shows that the third event (August 29 to September 8) is an excellent argument for defining a daily alongstream direction: the flow then was to the northwest (Fig. 1b), yet according to T_{575} and corroborating evidence from the NOAA/NESS satellite pictures, this flow was indeed the Gulf Stream. In fact, the top-to-bottom coherence of Gulf Stream flow is more apparent in Fig. 1c than 1a. The baroclinicity of the alongstream flow is obscured due to the changing velocity scales with depth, which were chosen so that the 4000 m velocities, e.g., would in fact be discernible. However, note that all the scales on the cross-stream

velocities are the same, emphasizing the depth-independence of the cross-stream velocities: this feature would never have been isolated in strictly east-north coordinates.

To quantify the baroclinic and barotropic structures of the along- and cross-stream velocities, empirical orthogonal functions (EOFs) for their vertical structures were computed. Time series from the standard depths were used, and EOFs were computed using data from the four complete (360-day) records. EOFs may be computed for the separate velocity components as well as for the vector velocity as a function of depth. If there is a strong coupling between the two components, the structure of the latter may be considerably different than the structure obtained by adding the EOF structures for the individual components. The EOFs were computed both ways and compared, but no such differences were found, indicating that there is little coupling between along- and cross-stream velocity components. The correlation coefficient for the two time series of amplitude, for the two dominant modes of the separate components, attains a maximum value of $C = 0.1$, when the cross-stream series is not lagged at all. For an estimated 30 degrees of freedom, C must be ≥ 0.3 for a significant correlation at the 95% confidence level. (The number of degrees of freedom was estimated by calculating the autocorrelation function for a given time series and finding the first zero crossing, which usually occurred from 7 to 15 days: for a time series of 360 days, that implies ~ 30 degrees of freedom.) Only calculations for the separate components are described here. Note that when data are available at N points in the vertical, N EOFs will be computed.

When data from the 575, 875, 2000 and 4000 db records are used, 92.4 percent of the variance in cross-stream velocity is accounted for by the first mode, with the vertical structure shown in Fig. 2a. Notice how nearly depth-independent the mode is. The second, third and fourth modes contain, respectively, 5.9, 1.7 and 0.03 percent of the variance and are thus of little importance in comparison to the first mode. The fourth mode contains essentially zero variance, as it must be because as pointed out two paragraphs ago, the definition of cross-stream removes one degree of freedom in the

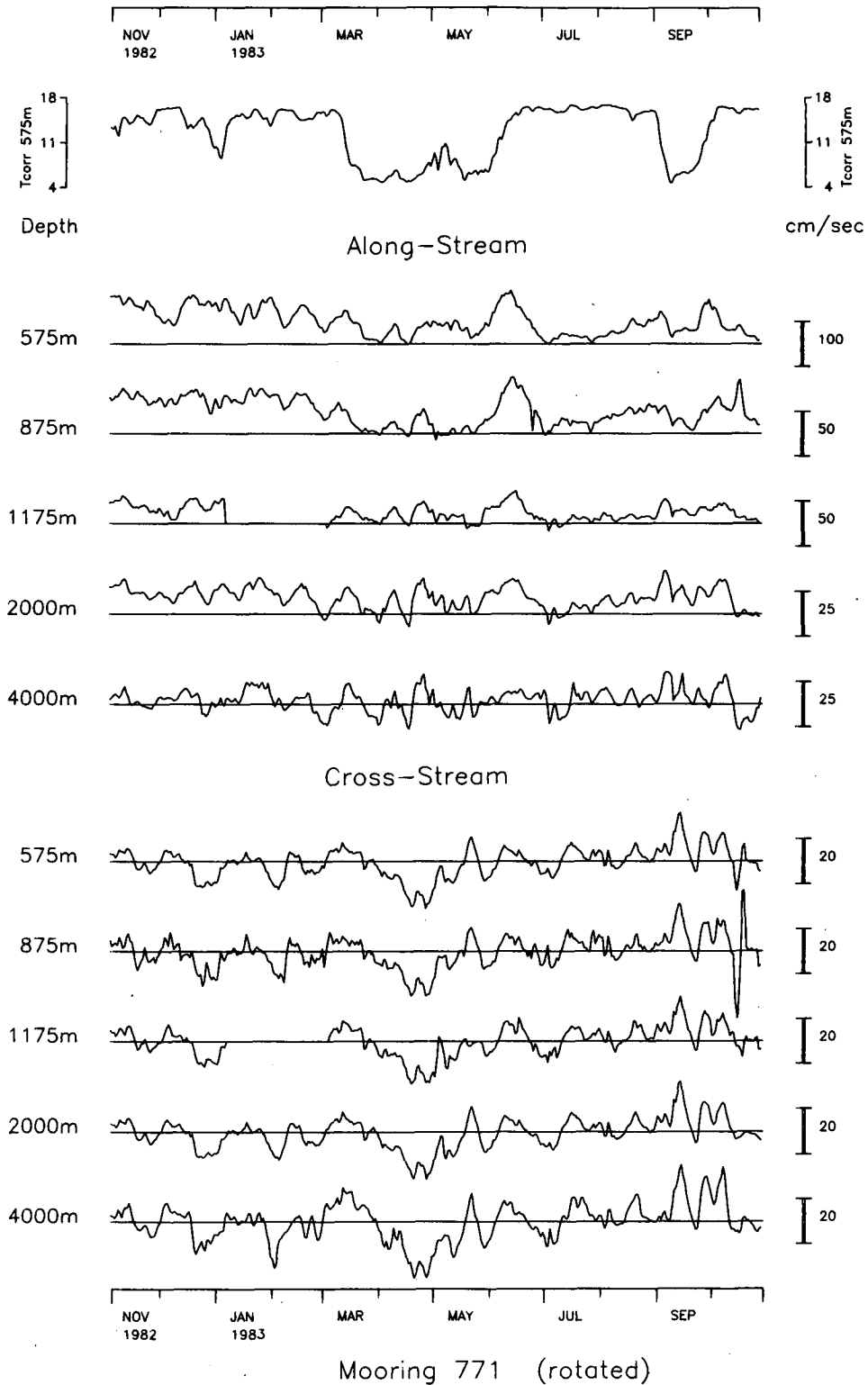


FIG. 1. (Continued)

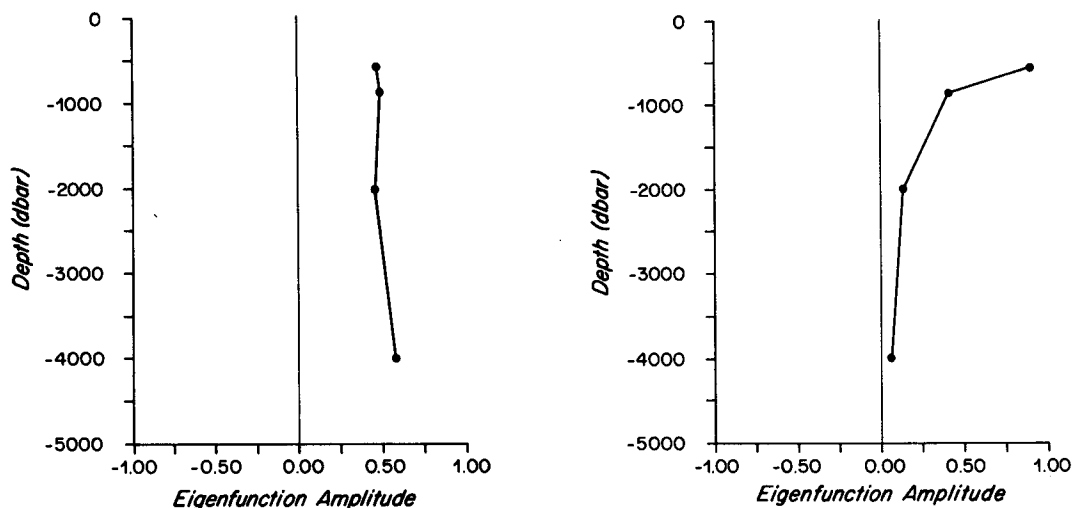


FIG. 2. Vertical structure of the first EOF calculated (a) for cross-stream velocity, and (b) for alongstream velocity, using complete (360 day) records at four depths.

vertical for this component. In the alongstream direction, the first calculated EOF accounts for 89.8 percent of the variance, and has the strongly baroclinic vertical structure shown in Fig. 2b. There is no reversal of the amplitude at 4000 m, indicating that the time-varying deep flow in these coordinates is statistically in the same direction as the thermocline flow. The second, third and fourth modes contain 6.2, 3.7 and 0.3 percent of the energy, respectively.

Table 2 shows the mean statistics for the velocities in the rotated coordinate system. The mean along-stream velocities are stronger by 50 to 100 percent than the mean east velocities throughout the water column, and are in the same direction top to bottom. The cross-stream velocity variance is practically barotropic, and the total EKE throughout the water column constitutes a smaller proportion of the total kinetic energy for these coordinates, indicating that much of the EKE calculated in Table 1 is associated with the meandering of the Gulf Stream rather than changes in its inherent structure.

In summary, the successful definition of an along-stream flow direction leads to a clean description of the flow's vertical structure at the mooring site. In the rotated coordinates, the fluctuations, as well as the

mean, break down neatly into a baroclinic alongstream mode and a barotropic cross-stream mode, which are decoupled, and each of which contains about 90 percent of the variance. Furthermore, the structure of both the mean and fluctuating alongstream mode show no flow reversals at depth, indicating that the Gulf Stream as defined here does indeed penetrate to the bottom.

4. Horizontal structure of the Gulf Stream

The meandering of the Gulf Stream back and forth past the mooring site suggests that a horizontal description of the Stream might be deduced from the mooring data, to complement the vertical description. A scatter plot of alongstream velocity versus temperature at 575 db (Fig. 3) shows that the former is a strong function of the latter. If the cross-stream temperature structure at 575 db remains fairly constant in time (though it may meander about), then at any given time the corrected temperature at 575 db ought to indicate how far in the cross-stream direction the mooring is located relative to the axis of the alongstream flow. Johns (1985) has recently shown that the primary mode of displacement of the thermocline in the Gulf Stream is a strict translation of the isotherms, rather than either a tilting or squeezing, for example. Thus, as a first approximation, this assumption of fixed cross-stream structure is justified. The much longer scales of variation in the downstream direction prevent a similar approach for a description of alongstream flow structure, which will henceforth rarely be discussed.

Hall and Bryden (1985) give a brief exposition of how the functional relation between temperature and cross-stream distance may be quantified, reiterated here for the reader's convenience. Consider Fig. 4, which shows a scatter plot of $\partial T / \partial \hat{y}$ as a function of T at 575 db, where the $\hat{\cdot}$ notation refers to rotated coordi-

TABLE 2. Record-length statistics for velocities in rotated coordinate system at standard depths.

Depth (db)	\bar{u} (cm s ⁻¹)	\bar{v} (cm s ⁻¹)	\bar{u}^2 (cm ² s ⁻²)	\bar{v}^2 (cm ² s ⁻²)
575	51.003	-.600	918.60	45.01
875	25.020	-.448	248.67	56.55
1175	11.942	-.027	77.17	45.09
2000	8.852	-.638	36.48	44.67
4000	2.118	-.147	37.72	75.15

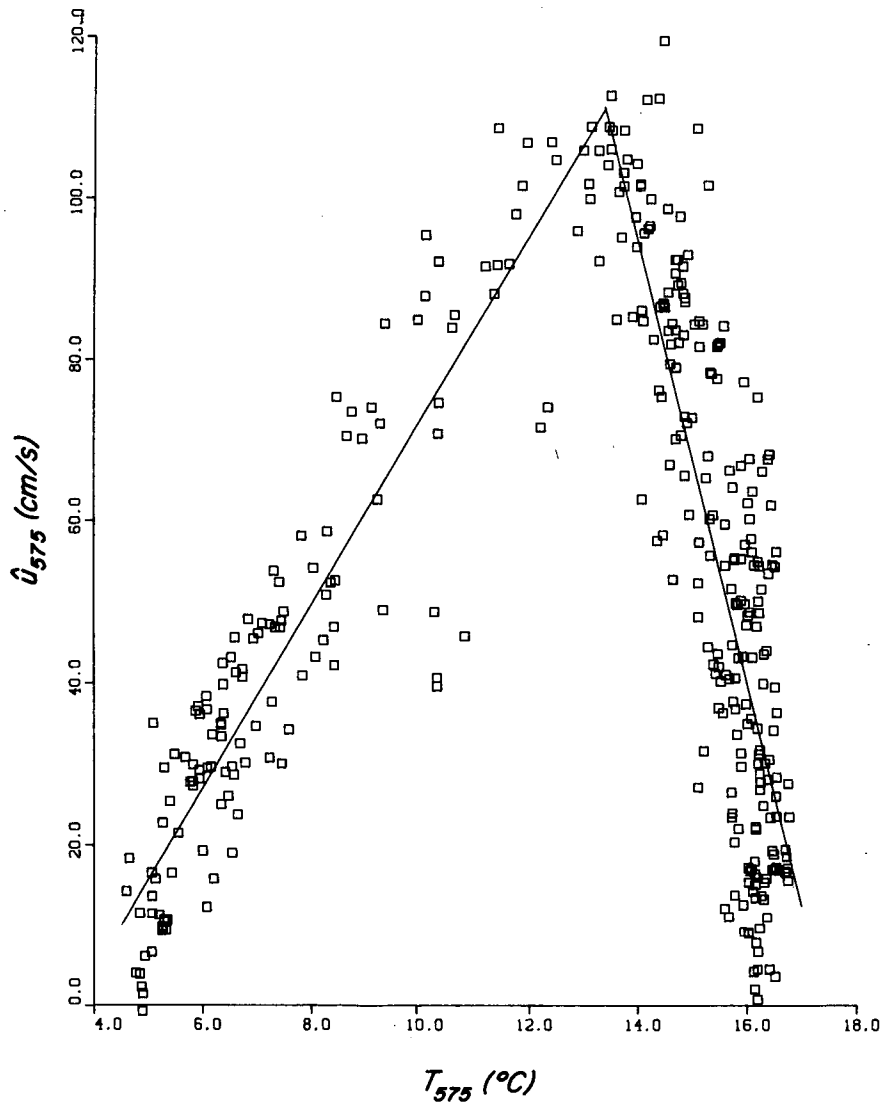


FIG. 3. Scatter plot of \hat{u} vs T at 575 db, along with linear least squares fit from (4a, b). For neatness' sake, the two lines defined by (4a, b) are drawn to intersect at $T = 13.4$, where (4a, b) give the same value of \hat{u} .

nates (see schematic sketch Fig. 5). With thermal wind ($\rho_0 f \partial \hat{u} / \partial z = g \partial \rho / \partial \hat{y}$) and the assumption that salinity is a function of temperature alone such that $d\rho = -\alpha_0 dT$ where $-\alpha_0 = \partial \rho / \partial T + (\partial \rho / \partial S)(dS/dT)$, the cross-stream temperature gradient at 575 db may be obtained from the measured velocities and pressures at the 400 and 700 m instruments. Since rotated velocities were used, technically $(f + \partial \alpha / \partial t)$ ought to be used in place of f in the geostrophic relation, where α is the daily-defined streamwise direction; however α_t is generally several orders of magnitude less than f , and so it can be ignored. The points were divided into two categories, those for which $T_{575} > 13^\circ\text{C}$ or $T_{575} < 13^\circ\text{C}$, and least squares linear fits were obtained for $T_{\hat{y}}$, which are also shown. The exact forms for the two lines are

$$T < 13^\circ\text{C}: \quad \frac{\partial T}{\partial \hat{y}} = 0.0885^\circ\text{C km}^{-1} - 0.0244 \text{ km}^{-1} \times T; \tag{1a}$$

$$T > 13^\circ\text{C}: \quad \frac{\partial T}{\partial \hat{y}} = -1.004^\circ\text{C km}^{-1} + 0.0602 \text{ km}^{-1} \times T. \tag{1b}$$

If $\hat{y} = 0$ for $T = 13^\circ\text{C}$, (1a, b) may be integrated in either direction to obtain $T = T(\hat{y})$, and inverted to obtain $\hat{y} = \hat{y}(T_{575})$. The results are

$$T < 13^\circ\text{C}: \quad T = 3.630^\circ\text{C} + 9.370^\circ\text{C} e^{-0.0244 \hat{y} / \text{km}} \tag{2a}$$

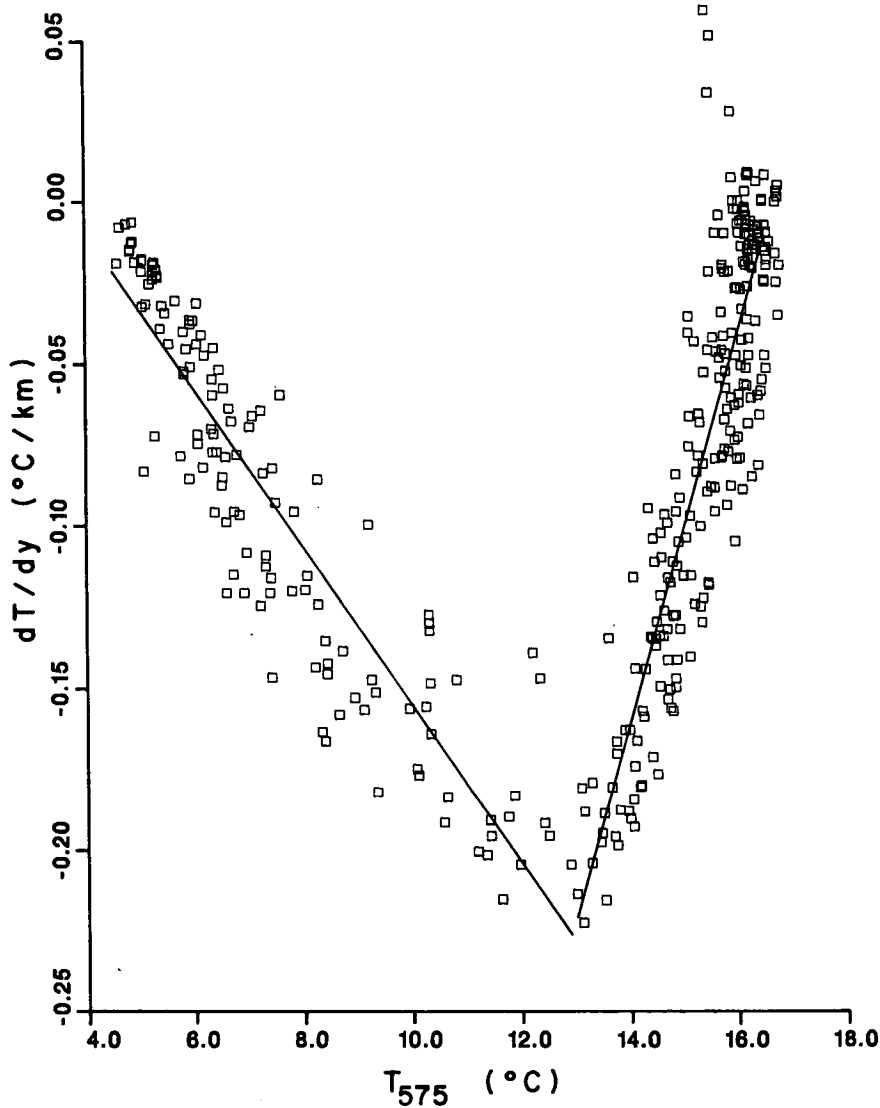


FIG. 4. Scatter plot of $\partial T/\partial \hat{y}$ vs T at 575 db, along with linear least squares fit.

$$\hat{y} = \frac{-km}{0.0244} \ln \frac{0.0885^\circ\text{C km}^{-1} - .0244 \text{ km}^{-1} T}{-0.228^\circ\text{C km}^{-1}} \quad (3a)$$

$T > 13^\circ\text{C}$:

$$T = 16.670^\circ\text{C} - 3.670^\circ\text{C} e^{.0602\hat{y}/km} \quad (2b)$$

$$\hat{y} = \frac{km}{0.0602} \ln \frac{1.004^\circ\text{C km}^{-1} - .0602 \text{ km}^{-1} T}{0.221^\circ\text{C km}^{-1}} \quad (3b)$$

At depths greater than 575 db, there is not such a strong and clear dependence of the shear (and hence $T_{\hat{y}}$) on temperature, making any other level less suitable for this procedure than is the 575 db level.

A linear least squares fit of alongstream velocity \hat{u}_{575} to T_{575} :

$T < 13^\circ\text{C}$:

$$\hat{u}_{575} = -40.951 \text{ cm s}^{-1} + 11.332 \text{ cm s}^{-1} \text{ }^\circ\text{C}^{-1} \times T \quad (4a)$$

$T > 13^\circ\text{C}$:

$$\hat{u}_{575} = 479.35 \text{ cm s}^{-1} - 27.463 \text{ cm s}^{-1} \text{ }^\circ\text{C}^{-1} \times T \quad (4b)$$

may be combined with Eqs. (2) to obtain a qualitative description of velocity in the thermocline:

$T_{575} < 13^\circ\text{C}$:

$$\hat{u}(\hat{y}) = \hat{u}(\hat{y} = 0) + 106.19 \text{ cm s}^{-1} (e^{-0.0244\hat{y}/km} - 1) \quad (5a)$$

$$\frac{\partial \hat{u}}{\partial \hat{y}} = -0.259 \times 10^{-4} \text{ s}^{-1} e^{-.0244\hat{y}/km} \quad (6a)$$

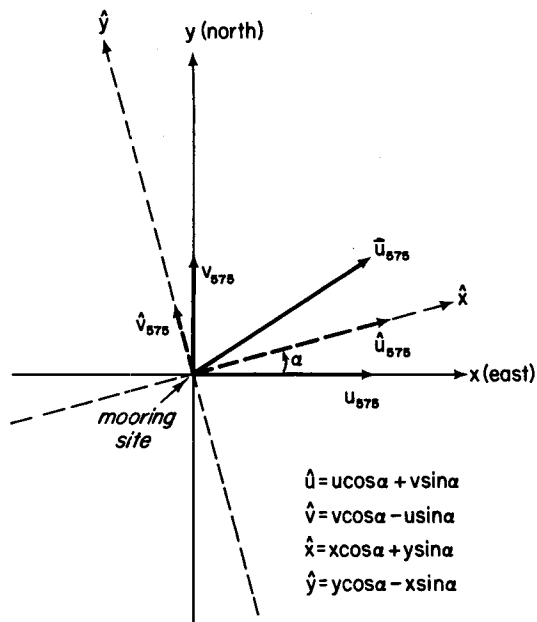


FIG. 5. Schematic showing coordinate rotation and transformation definitions.

$T_{575} > 13^\circ\text{C}$:

$$\hat{u}(\hat{y}) = \hat{u}(\hat{y} = 0) + 100.78 \text{ cm s}^{-1} (e^{0.0602\hat{y}/\text{km}} - 1) \quad (5b)$$

$$\frac{\partial \hat{u}}{\partial \hat{y}} = 0.607 \times 10^{-4} \text{ s}^{-1} e^{0.0602\hat{y}/\text{km}}. \quad (6b)$$

These fits are rather simplistic, and imply discontinuities in $\hat{u}_{\hat{y}}$ and $T_{\hat{y}}$ at the stream axis. They are not expected to reproduce details of the flows, and are applied only mechanically in the analysis.

The results (5), (6) imply that the warm, anticyclonic side of the stream is actually sharper than the cold, cyclonic side in the sense that

$$\left| \frac{\partial \hat{u}}{\partial \hat{y}} \right|_{T_{575} > 13^\circ\text{C}} > \left| \frac{\partial \hat{u}}{\partial \hat{y}} \right|_{T_{575} < 13^\circ\text{C}},$$

in fact nearly three times as sharp. This result contradicts conventional wisdom (e.g., see Fofonoff and Hall, 1983) that the northern edge of the Stream, in analogy with the two-layer inertial jet model, should exhibit a much more sudden jump in velocity than the warm side. It may be that the structure proposed by Fofonoff and Hall is found higher up in the water column. The North Wall of the Gulf Stream, defined as the place where the 15°C isotherm is at 200 m depth (Fuglister, 1963) has long been used as an indicator of Gulf Stream position, but clearly that is well above the depth range detectable by the mooring. Analysis of the Pegasus sections at 73°W by Halkin and Rossby (1985) shows that instantaneously as well as on average the horizontal velocity shear is much stronger on the cold than on

the warm side in the upper few hundred meters; even at 600 m depth, though less pronounced, the same trend is definitely there. The velocity section constructed by Warren and Volkmann (1968), on the other hand, gives a general impression that $\partial \hat{u} / \partial \hat{y}$ is stronger on the warm side, but at 600 m depth the shear appears to be nearly symmetric about the maximum along-stream velocity at that depth.

Possibly the error involved in a “frozen field” assumption could affect the inferred horizontal shear on either side of the stream axis. This error is one of the most difficult to assess with a single mooring, but some discussion is provided at the end of the next subsection. In a forthcoming paper, Hall (1986) explores the likelihood that the stream does in fact experience changes in width in the presence of meandering: Chew (1974) found that to be the case in the Florida Current, based on a study of XBT data and parachute drogues. It is not clear how such changes would affect the relative shear strengths, and more data will be required to resolve this question.

Horizontally integrated fluxes. Time may be used parametrically, with $\hat{u} = \hat{u}(t)$ and $\hat{y} = \hat{y}[T(t)]$, to integrate streamwise fluxes horizontally as well as vertically for the four events when the Gulf Stream swept by the mooring. Hall and Bryden (1985) have tabulated and briefly discussed the mass transports resulting from this calculation. Here the four events are considered in greater detail. Since the data only extended upward as far as 575 db, and since much of the transport is known to occur above that depth, some extrapolation scheme was required to extend velocities to the surface. Different schemes were tested on hydrographic data from Gulf Stream '60 at 68.5°W to determine which one best reproduced the actual shear in the upper water column, and that chosen is probably somewhat conservative. In particular, if (u_4, P_4) and (u_7, P_7) are the measured alongstream velocities and pressures at the 400 and 700 m instruments respectively, a value of

$$u_1 = u_4 + S(u_4 - u_7), \quad S = \frac{1}{2} \quad (7)$$

was assigned to the level $P_1 = 2P_4 - P_7$ (linear extrapolation), and this value was considered to be constant to the surface. At the bottom, the velocity was assumed to decrease linearly from its value at 4000 m to zero at the bottom depth of 4688 m. The actual measured velocities and pressures were used since these are depth-integrations, not requiring standard levels.

Table 3 gives the pertinent information for the four events, which divide themselves more or less into two categories. In March and early September, T_{575} was decreasing, indicating that the translational cross-stream velocity of the flow was negative (southward-like); yet the average measured cross-stream velocities for those two events were positive (see Fig. 1c, bottom).

TABLE 3. Summary of main features of four Gulf Stream passages across GUSTO mooring site, with values from Section 1 of the Gulf Stream 60 survey included for comparison. Axis velocity is the maximum velocity attained during an event. Other features are described in the text.

Dates of event (1983)	Range of T_{575} (°C)	Width (km)	Axis velocity (cm s ⁻¹)	Mass transport (10 ⁶ m ³ s ⁻¹)	Momentum flux (10 ⁹ N)	Kinetic energy flux (10 ⁹ J s ⁻¹)
6–25 Mar	16.017–5.068	105.5	74.6	83.9	44.6	16.9
26 May–21 Jun	6.000–16.442	102.6	119.5	115.5	75.7	35.3
29 Aug–8 Sep	15.892–5.673	88.2	71.5	96.6	41.9	13.1
11 Sep–5 Oct	5.395–16.386	109.7	99.5	111.0	62.3	27.3
Gulf Stream 60 Sect. 1	5.70–?	111.1		98.2	89.4	60.7

In June and late September, translational velocities were positive, and so were the average measured cross-stream velocities. The maximum velocities at 575 db for the former two events are considerably lower than for the latter two (about 20–30 cm s⁻¹), yet mass transport is correspondingly lower only for the March event, if the narrower width of the early September passage is taken into account. A glance at Fig. 1c shows that strong alongstream velocities at 4000 m in early September are associated with the difference. The values in Table 3 are similar to Fuglister’s (1963) estimate of Gulf Stream transport at 68.5°W of $136 \times 10^6 \text{ m}^3 \text{ s}^{-1}$, and Warren and Volkmann’s (1968) estimate at 38°N, 69°W of $101 \times 10^6 \text{ m}^3 \text{ s}^{-1}$.

The Gulf Stream is profiled either as a meander propagates over the mooring site, or as the Stream structure (perhaps convoluted in a meander) is advected past the mooring. The conceptual difference between the two possibilities is that the latter could occur as a result of an ambient velocity field outside the Stream “pushing” the meander along. In this case, the transport estimates made from the current meter data can be altered substantially by the existence of the ambient field, because without explicit knowledge of what the ambient velocity is, it is impossible to separate it from the velocity structure of the Stream itself. The projection of the ambient velocity onto the alongstream direction can then augment the transport estimate for an event as follows: suppose the ambient field is zonal, while the stream is directed at an angle α to due east. Then the apparent transport will exceed the actual Gulf Stream transport (which would be measured if one could move with the meander) by an amount

$$\Delta T = u_{\text{amb}} \cos \alpha \Delta y \Delta z$$

which for $u_{\text{amb}} = 5 \text{ cm s}^{-1}$, $\alpha = 45^\circ$, $\Delta y = 100 \text{ km}$ and $\Delta z = 4000 \text{ m}$ is

$$\begin{aligned} \Delta T &= 5 \times 10^{-2} \text{ cm s}^{-1} \times \frac{2^{1/2}}{2} \times 10^5 \text{ m} \times 4 \times 10^3 \text{ m} \\ &= 14 \times 10^6 \text{ m}^3 \text{ s}^{-1}, \end{aligned}$$

which is comparable to the transport differences between the various Gulf Stream events. Of course, the situation may be more complicated than described

above. The possibility that there are detached rings interacting with the Stream, or that the Gulf Stream axis is in fact extensible, could introduce complicating factors in trying to interpret observations from a single point.

Integrated momentum and kinetic energy fluxes have also been calculated and are listed in Table 3. For comparison, values from Section I of Gulf Stream ’60 (Fofonoff and Hall, 1983) are also presented. The June event most resembles the flow that was surveyed in Gulf Stream ’60, in terms of total fluxes. The extrapolation scheme to the surface for the GUSTO data may be somewhat conservative, yet it is in the upper water that the greatest contributions to momentum and kinetic energy fluxes arise. That may explain why the mass transport is estimated reasonably well, while the momentum and kinetic energy transports seem to be underestimated. For example, if the value of the shear S is increased to 1 in (7), calculated mass transports increase by only 5–7 percent, while momentum transports increase by 20–30 percent and kinetic energy transports by 50–65 percent. It is also possible that the fluxes would agree more closely with Gulf Stream ’60 data if, e.g., some sort of exponential rather than linear extrapolation scheme were used for the surface waters. Although estimates of mass transports would not be changed very much, again momentum and kinetic energy fluxes could change dramatically because they depend on higher moments of alongstream velocity.

Aside from the choice of extrapolation scheme, the primary source of error in the transport calculations is that involved with obtaining the cross-stream coordinate \hat{y} . The error in estimated horizontal width is most important where the alongstream velocities are large, since that is where the greatest transport contributions occur. To the extent that $\partial T / \partial \hat{y}$ is not an absolutely fixed function of T_{575} , as assumed, errors for the different transport events can arise. Although with just one mooring it is impossible to evaluate the possible tilting or squeezing of isotherms at 575 db, the scatter of the actual values of $\partial T / \partial \hat{y}$ about the linear fits should be some indication of the inherent error in the “fixed form” Gulf Stream assumption. For the range $T_{575} < 13^\circ\text{C}$, the rms difference between the actual values of $\partial T / \partial \hat{y}$ and the linear fit is $2.31 \times 10^{-2} \text{ }^\circ\text{C km}^{-1}$; the

value of $\partial T/\partial y$ at $T_{575} = 10^\circ\text{C}$ (where alongstream velocities become moderately large) is $-0.155^\circ\text{C km}^{-1}$, and at $T_{575} = 13^\circ\text{C}$ (the stream axis), about $0.23^\circ\text{C km}^{-1}$; thus possible errors in cross-stream width on the order of 10 to 15 percent are anticipated. For $T_{575} > 13^\circ\text{C}$, the rms difference is $3.01 \times 10^{-2}^\circ\text{C km}^{-1}$, and $\partial T/\partial y$ at $T_{575} = 15^\circ\text{C}$ is $0.101^\circ\text{C km}^{-1}$, leading to errors on the order of 13–30 percent for y on the warm side of the stream. Notice that the errors are expected to be least at the stream axis, where alongstream velocities are strongest, because $\partial T/\partial y$ is largest there. A small error is involved in the assumption of constant $\alpha_0 = -d\rho/dT$ to evaluate $\partial T/\partial y$ from the shear: at 575 db, this parameter varies by less than 10 percent. Overall errors for the integrated mass fluxes are estimated to be 20–25 percent.

5. Vertical velocities at the mooring site

To complete the picture of the velocity field at the mooring site, time series of vertical velocity at all depths have been calculated. Following Bryden (1980), the temperature equation may be written

$$\frac{\partial T}{\partial t} + \frac{\rho_0 f}{g\alpha_0} R^2 \frac{\partial \phi}{\partial z} + w \frac{\partial \theta}{\partial z} = \text{rhs}$$

where $u = R \cos \phi$, $v = R \sin \phi$, R is the current speed and $\phi = \tan^{-1}(v/u)$ is the angle the velocity vector makes with east; θ is potential temperature. Under an assumption of negligible mixing (i.e., rhs is small), vertical velocities may be calculated from

$$w = -\left(\frac{\partial T}{\partial t} + \frac{\rho_0 f}{g\alpha_0} R^2 \frac{\partial \phi}{\partial z} \right) / \left(\frac{\partial \theta}{\partial z} \right). \quad (8)$$

Equation (8) uses thermal wind to replace temperature gradients with velocity shears; Hall (1985) has discussed the validity of the geostrophic approximation at the mooring site and concludes that it is valid to within 20 percent at 575 db, and to within less than 10 percent at greater depths.

With slight variations to accommodate the data at each depth (see Hall, 1985, for a detailed account), (8) was used to calculate vertical velocities at all depths but 4000 m. The numerator was calculated from the data; to avoid introducing more noise by calculating θ_z from the recorded data, the analytic fits used in the temperature correction schemes at 575, 875 and 1175 db were used. At 2000 db, a constant value of $0.0971^\circ\text{C}/100\text{ m}$ (determined from historical data) was used. At 4000 m, there is a lack of vertical information to compute w using the temperature equation; however, since this current meter was only 688 m off the bottom, a fair idea of the deep vertical velocities may be obtained by calculating $w_{4000} = \mathbf{u} \cdot \nabla h$, where ∇h is the slope of the bottom topography. At the time of mooring recovery, a bathymetric survey was conducted about the mooring site; the survey indicated a slope of 4

$\times 10^{-3}$, with alongslope directed along 70° true. It should be emphasized that the calculation of deep vertical velocity is absolutely independent of all those calculations made higher in the water column.

The resulting time series of w at the five depths are displayed in Fig. 6, after being smoothed with a five-day running mean (except at 4000 m, where the time-series was already fairly smooth). The vertical velocities exhibit good visual coherence throughout the water column, and calculating correlation coefficients for pairs of series bears out what is evident from the plots—that vertical velocities are indeed well correlated throughout the water column. Table 4 lists the correlation coefficients, all of which are significant at the 95% confidence level for an estimated 30 degrees of freedom. Table 4 also shows the mean and rms values of w at the five levels. The mean values of the vertical velocities are an order of magnitude smaller than the rms values, and probably not significantly different from zero. Because time-varying quantities contribute to the record-length means, the latter are not less than zero throughout the water column, as the presence of the mean horizontal velocity field alone would imply (see section 2). The contributions of local temperature change and horizontal advection to the vertical velocity variance are roughly equal in magnitude. The maximum rms amplitude of 0.08 cm s^{-1} is attained mid-depth, at 875 db; a close look at the time series reveal that instantaneously w_{max} occurs at thermocline levels, which vary from 875 db on the warm side of the stream to 575 db on the cold side. The monotonic decay above and below the thermocline maximum appears in the first EOF for the vertical structure of vertical velocity, which contains 81.9 percent of the variance and looks like the vertical velocity structure associated with the first baroclinic mode (Fig. 7). This result, taken with the neat decoupling of horizontal velocities into just two modes, suggests that a two-layer model (which reproduces a barotropic and baroclinic mode) can adequately describe the data.

There is an important connection between the vertical velocities and the results noted in Table 3, that inferred translational and measured cross-stream velocities do not always have the same sign. If we suppose that the cross-stream contribution $\hat{v}T_y$ dominates the alongstream contribution $\hat{u}T_x$ in the temperature equation, then opposing translational and measured cross-stream velocities simply imply that horizontal advection does not balance local temperature change, and vertical velocities must exist. In fact, the calculation of w from (8) depends not at all on the definitions of along- and cross-stream, but only on how the velocity vector turns with depth. When strong vertical velocities are estimated, then, it is to be expected that horizontal advection is not compensating but reinforcing local temperature changes: at these times, one might anticipate opposing translational and measured cross-stream velocities. That is indeed the case for the March and

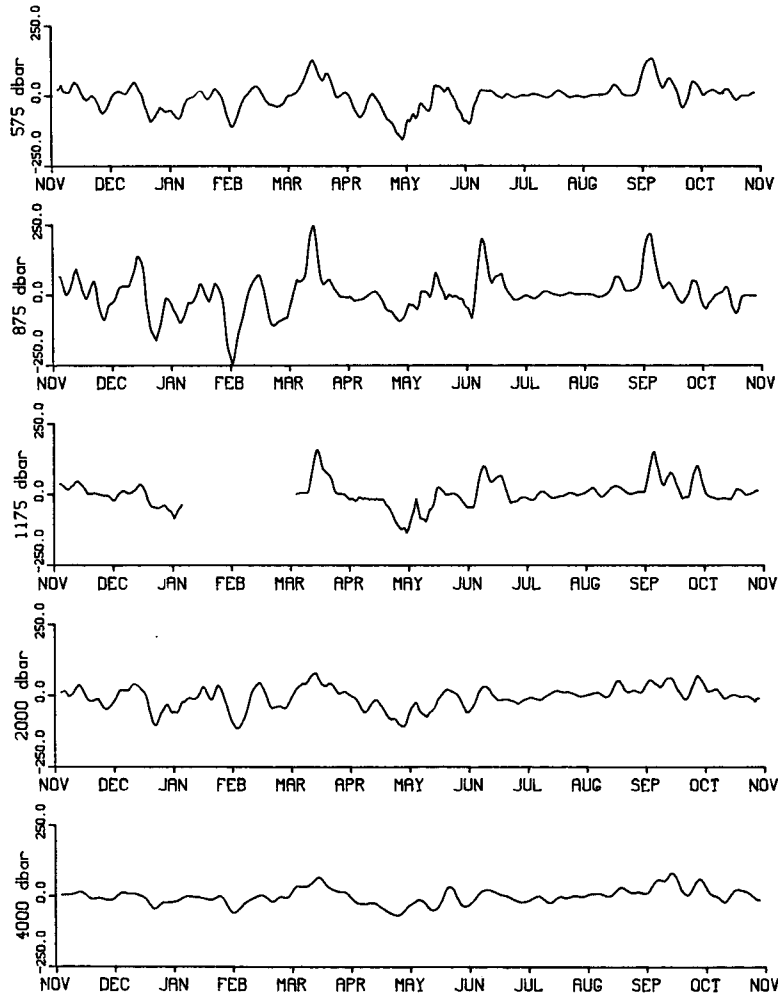


FIG. 6. Vertical velocities at designated levels, calculated as described in text. From top to bottom are vertical velocities at 575, 875, 1175, 2000 and 4000 db. Units are $10^{-3} \text{ cm s}^{-1}$.

TABLE 4. Top: Record-length mean and rms velocities for vertical velocities calculated as described in text. Value at 1175 dbar is based on 240 days of data, the rest on 360 days. Bottom: Correlation coefficients for different pairs of vertical velocity, $C_{w_i w_j} = \overline{w_i w_j} / (\overline{w_i^2} \overline{w_j^2})^{1/2}$.

Depth (db)	\bar{w} ($10^{-3} \text{ cm s}^{-1}$)	w_{rms} ($10^{-3} \text{ cm s}^{-1}$)			
575	-4.38	54.66			
875	3.50	83.86			
1175	3.45	56.15			
2000	-6.73	44.24			
4000	-0.90	29.32			
	w_{875}	w_{1175}	w_{2000}	w_{4000}	
w_{575}	0.73	0.74	0.80	0.69	
w_{875}		0.62	0.68	0.52	
w_{1175}			0.64	0.70	
w_{2000}				0.78	

early September crossing (Fig. 6); w is moderately smaller during the June crossing, and much smaller in late September. These aspects of the flow, and their implications for the underlying dynamics, are further explored in Hall (1986).

6. Discussion of quasi-geostrophic approximation

In quasi-geostrophic theory, the Rossby number ϵ is defined as U/fL (where U is a velocity scale and L a horizontal length scale), a measure of the strength of advection relative to the Coriolis terms in the momentum equations, or of relative to planetary vorticity. For a strongly nonisotropic flow like the Gulf Stream, there will be a different estimate for each momentum equation—for the alongstream direction $\epsilon_x \sim U/fL_y$ and for the cross-stream $\epsilon_y \sim V/fL_x$. If $U \gg V$ and $L_x \gg L_y$, clearly $\epsilon_x \gg \epsilon_y$. As long as $\epsilon_x \ll 1$, however, quasi-geo-

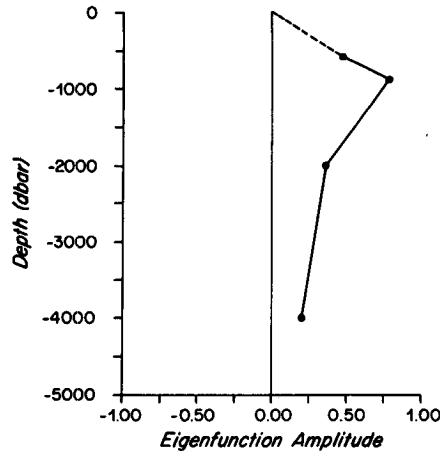


FIG. 7. Vertical structure of the first EOF calculated for vertical velocity from complete (360 day) records at four depths. The dashed line goes to $w = 0$ at the surface, which is the boundary condition there.

strophic theory still applies, because all nondimensional variables can be formally expanded in a power series of ϵ_x , leading to the derivation of the quasi-geostrophic potential vorticity equation (see Pedlosky, 1979). The Rossby number crops up repeatedly as a limit on the relative size of other flow attributes, such as vertical velocities or isotherm slopes. Several estimates of ϵ_x from the data are presented here to demonstrate that perhaps quasi-geostrophic scaling should be replaced, e.g., by frontal (or semigeostrophic) scaling when modeling the Gulf Stream. The subscript x is dropped for convenience: all estimates are implicitly of ϵ_x , since what is important is the upper bound on the Rossby number.

When the mooring is in the Gulf Stream, velocities range well over 100 cm s^{-1} at 575 db (see Fig. 1c); the scale of cross-stream variation is about 50 km, from the fits (5, 6). Thus, the definition $\epsilon = U/fL_y$ gives

$$\epsilon \sim \frac{100 \text{ cm s}^{-1}}{0.89 \times 10^{-4} \text{ s}^{-1} \times 50 \text{ km}} = 0.22.$$

The vertical velocity calculations of section 5 yielded maximum rms magnitudes at 875 db of 0.08 cm s^{-1} and 0.05 cm s^{-1} at 575 db (Johns and Watts, 1985, recently estimated similar values of vertical velocity in the Gulf Stream 100–200 km northeast of Cape Hatteras). A scale analysis of the continuity equation shows that according to quasi-geostrophic theory, in order that the horizontal velocity remain nondivergent to lowest order in ϵ ,

$$\frac{U}{L_x} \sim \frac{V}{L_y}, \quad \frac{W}{H} \sim \epsilon \left(\frac{U}{L_x}, \frac{V}{L_y} \right)$$

where (U, L_x) , (V, L_y) denote along- and cross-stream (velocity, length) scales, and (W, H) the corresponding vertical scales. For the Gulf Stream, typical scales are

$U = 100 \text{ cm s}^{-1}$, $V = 5 \text{ cm s}^{-1}$, $L_x = 1000 \text{ km}$, $L_y = 50 \text{ km}$, $H = 1 \text{ km}$, and $w = 5 \times 10^{-2} \text{ cm s}^{-1}$. Then $\epsilon \sim WL_x/UH \sim WL_y/VH = (0.05 \text{ cm s}^{-1})(100 \text{ km})/(10 \text{ cm s}^{-1})(1 \text{ km}) = 0.5$. This estimate is essentially an indication of the strong isotherm slopes in the Gulf Stream. In particular, quasi-geostrophic scaling of the temperature equation, assuming local time derivatives do not dominate, gives

$$\frac{\partial z}{\partial y} \Big|_T \sim \frac{\partial T / \partial y}{\partial \theta / \partial z} \sim \frac{w}{\bar{v}} \sim \frac{\epsilon VH / L_y}{V} = \frac{\epsilon H}{L_y}.$$

In these relations, H is meant to be the vertical scale of variation, e.g., for the horizontal velocities. Quasi-geostrophy requires that an isotherm not vary its depth an $O(1)$ amount within the length scales under consideration. However, an inspection of historical hydrographic sections (for example, see Fuglister, 1963) shows that

$$\frac{\partial z}{\partial y} \Big|_T \sim 10^{-2},$$

so that with $H = 1 \text{ km}$, and $L_y = 50 \text{ km}$, $\epsilon \sim 0.5$, the same estimate as that associated with vertical velocities.

These Rossby number estimates apply primarily to the flow at 575 db, that is, the thermocline Gulf Stream, and they range from 0.2 to 0.5. (Notice that the estimates depending on strong isotherm slopes are sensitive to the choice of H : if $H = 1.5 \text{ km}$, these estimates would be $\epsilon \sim 0.3$ instead of 0.5.) Deeper in the water column, similar estimates yield substantially lower Rossby numbers—all, that is, except for those derived from the vertical velocities, which are substantial throughout the water column (see Table 4). Below the 575 db level, thermal wind balance holds to within 10 percent in both the along- and cross-stream directions. At 575 db, using the geostrophic approximation probably introduces errors of about 20–30 percent, and certainly the errors would increase at still shallower levels. While thermal wind may be adequate for diagnostic calculations in the Gulf Stream relating temperature (or density) and velocity gradients, a Rossby number of about 0.3 suggests that a quasi-geostrophic dynamical model may be inadequate for predicting the time-evolution of the Gulf Stream.

7. Discussion

Now that it is technically feasible to collect long time series of current and temperature measurements throughout the water column in the Gulf Stream, our understanding of that current should advance dramatically. The GUSTO mooring was the first successful deployment of such a mooring, and the results from the data collected have revealed several features that may be useful in future investigations of the flow in this region. Analysis of the GUSTO data appears to justify the identification of the Gulf Stream primarily

as a discrete feature with a well-defined velocity structure, distinct from the measured Eulerian flow. Thus, a few well-placed moorings can provide considerable coverage of the stream, if use is made of temperature as a horizontal coordinate, and if a reasonable definition of flow direction is applied. Using the decomposition of velocities into their along- and cross-stream components shows that the vertical structure at the GUSTO mooring site is accounted for by a baroclinic alongstream mode and a decoupled, barotropic cross-stream mode. The inferred horizontal information may be used successfully to estimate mass transports of the Gulf Stream, which are relatively insensitive to the extrapolation scheme required to go from the thermocline to the surface. The current meter data have also been used to deduce the existence of strong vertical velocities in the Stream, with maximum rms values of 0.08 cm s^{-1} at thermocline levels, and a vertical structure resembling the first baroclinic mode. The large magnitudes of w and the associated large vertical divergence and vortex stretching suggest that a quasi-geostrophic dynamical framework is inadequate for describing this flow regime.

Certain types of information are required to clear up points that are left ambiguous by the GUSTO dataset. Data from the thermocline to the surface are needed to determine whether the velocity structure is sharper on the cyclonic or anticyclonic side. Also, the Rossby number has been estimated to be 0.2 or 0.3 at thermocline levels, but could possibly be larger at shallower levels where the relative vorticity $-u_y$ may be quite strong. More resolution of the shear above 575 db is required to pin down the estimates of momentum and kinetic energy transports. Finally, results from the GUSTO data have suggested that a two-layer system might adequately model stream dynamics; information on the velocity structure above the thermocline is necessary to determine whether or not two layers would be sufficient.

More than one mooring deployed in the cross-stream direction would be useful in addressing a variety of other issues. Transports could be monitored more accurately with more moorings across the stream, since it would take less time for the entire Stream to be profiled in a single passage over the sites; then it might be possible to determine whether transport really changes as dramatically in time as the GUSTO data suggest, or whether apparent changes are due to an ambient velocity field advecting features past the mooring site. It would also be possible to test the extent to which the stream maintains a constant width, further reducing the O(15–30 percent) errors in estimating mass transports.

The concept of the Gulf Stream as a discrete feature is not new; indeed, various theoretical investigations of its meandering and instability properties have been based on just such a scenario, beginning with the path prediction models of Warren (1963) and later contin-

ued with a model by Robinson and Niiler (1967). Luyten and Robinson (1974) and Robinson et al. (1975) have discussed the long-wavelength instabilities of a thin, quasi-geostrophic meandering jet assumed to move coherently from top to bottom. While in the past observational evidence to confirm the notion has been largely nonexistent, recently three new, different datasets have been employed to address this question: Johns (1985), using an array of inverted echo sounders at 73°W , demonstrated that 80 percent of the measured thermocline depth variance could be accounted for by a mode corresponding to uniform lateral displacement. Halkin and Rossby (1985) have used a set of 14 Pegasus sections across the Gulf Stream at 73°W to construct a composite Gulf Stream which, they show, is substantially different than simply averaging the velocity measurements of the individual Pegasus drops. Finally, the GUSTO dataset has been used to show how neatly much of the velocity structure can be accounted for if viewed in the proper frame. These approaches give rise to the most basic philosophical question that investigators must address in the future: when (if ever) is it appropriate to use Eulerian averages in examining regions of Gulf Stream flow? Our definitions of the general or time-averaged ocean circulation may have to be refined, that we may distinguish between an observable, Eulerian average circulation in the ocean, and the existence of a boundary current with an average structure but variable position and orientation, such that it affects the interior general circulation in order one fashion. It seems that observational tools are sufficiently advanced to resolve these philosophically different approaches in the near future.

Acknowledgments. This work was supported by grants OCE-8208746 and OCE-8500598 and a graduate fellowship from the National Science Foundation, and Contract N00014-82-C-0019, NR 083-004 from the Office of Naval Research. Many of the ideas in this work were stimulated by discussions with H. Bryden. N. Fofonoff, M. McCartney and W. Schmitz provided useful criticism and suggestions in the development of this work.

REFERENCES

- Bryden, H. L., 1980: Geostrophic vorticity balance in midocean. *J. Geophys. Res.*, **85**, 2825–2828.
- Chew, F., 1974: The turning process in meandering currents: A case study. *J. Phys. Oceanogr.*, **4**, 27–57.
- Fofonoff, N. P., and M. M. Hall, 1983: Estimates of mass, momentum, and kinetic energy fluxes of the Gulf Stream. *J. Phys. Oceanogr.*, **13**, 1868–1877.
- Fuglister, F. C., 1963: Gulf Stream '60. *Progress in Oceanography*, Vol. 1, Pergamon Press, 265–383.
- Halkin, D., and T. Rossby, 1985: The structure and transport of the Gulf Stream at 73°W . *J. Phys. Oceanogr.*, **15**, 1439–1452.
- Hall, M. M., 1985. Horizontal and vertical structure of velocity, potential vorticity and energy in the Gulf Stream. Ph.D. thesis, MIT/WHOI, WHOI-85-16, 165 pp.

- , 1986: Assessing the energetics and dynamics of the Gulf Stream at 68°W from moored current measurements. In preparation.
- , and H. L. Bryden, 1985: Profiling the Gulf Stream with a current meter mooring. *Geophys. Res. Lett.*, **12**, 203–206.
- Halliwell, G. R., Jr., and C. N. K. Mooers, 1983: Meanders of the Gulf Stream downstream from Cape Hatteras 1975–1978. *J. Phys. Oceanogr.*, **13**, 1275–1292.
- Johns, W. E., 1985: Dynamics and structure of Gulf Stream meanders northeast of Cape Hatteras, N.C. Ph.D. thesis, University of Rhode Island, 232 pp.
- , and D. R. Watts, 1985: Gulf Stream meanders: Observations on the deep currents. *J. Geophys. Res.*, **90**, 4819–4832.
- Luyten, J. R., 1977: Scales of motion in the deep Gulf Stream and across the Continental Rise. *J. Mar. Res.*, **35**, 49–74.
- , and A. R. Robinson, 1974: Transient Gulf Stream meandering. Part II: Analysis via a quasi-geostrophic time-dependent model. *J. Phys. Oceanogr.*, **4**, 256–269.
- Pedlosky, J., 1979: *Geophysical Fluid Dynamics*. Springer-Verlag, 624 pp.
- Raymer, M. E., A. Spencer and H. L. Bryden, 1986: Temperature correction for mooring motion on GUSTO current meter time series. WHOI Tech. Rep., in preparation.
- Richardson, P. L., 1983a: Eddy kinetic energy in the North Atlantic from surface drifters. *J. Geophys. Res.*, **88**, 4355–4367.
- , 1983b: A vertical section of eddy kinetic energy through the Gulf Stream System. *J. Geophys. Res.*, **88**, 2705–2709.
- Robinson, A. R., and P. P. Niiler, 1967: The theory of free inertial currents. I. Path and structure. *Tellus*, **19**, 269–291.
- , J. R. Luyten and G. Flierl, 1975: On the theory of thin rotating jets: A quasi-geostrophic time dependent model. *Geophysical Fluid Dynamics*, Vol. 6, Gordon and Breach, 211–244.
- Schmitz, W. J., Jr., 1984: Abyssal eddy kinetic energy in the North Atlantic. *J. Mar. Res.*, **42**, 509–536.
- Warren, B. A., 1963: Topographic influences on the path of the Gulf Stream. *Tellus*, **15**, 167–183.
- , and G. H. Volkman, 1968: Measurement of volume transport of the Gulf Stream south of New England. *J. Mar. Res.*, **26**, 110–126.